

# Residual stresses in multi-pass butt-welded ferritic-pearlitic steel pipes

N. Hempel · Th. Nitschke-Pagel · K. Dilger

Received: 18 August 2014 / Accepted: 4 February 2015 / Published online: 17 February 2015  
© International Institute of Welding 2015

**Abstract** This study is dedicated to the investigation of the residual stress development in multi-pass butt-welded joints of ferritic-pearlitic steel pipes. Therefore, temperature profiles are taken during welding, and the residual stresses are determined by X-ray diffraction measurements on the outer and inner surfaces of the pipes. The distortion of the specimens is measured by laser triangulation. In order to identify the influence of the tubular geometry in contrast to a plane one, plates are welded with the same parameters, and the results are compared. The residual stress distributions in both pipes and plates can be explained by phase transformations and thermal contraction. However, it is shown that the latter is the governing mechanism in the residual stress development in the pipes considered in this study, which is due to their distinct geometry.

**Keywords** Residual stresses · Steels · Tubes and pipes

## 1 Introduction

Residual stresses generally can have diverse effects on the structural performance of welded components. Tensile residual stresses usually reduce their fatigue life whereas compressive stresses have a converse effect. Therefore, the knowledge of residual stresses is needed for the design of both safe and efficient components. However, the results of numerical

computations of welding residual stresses strongly depend on the material model used in the simulations [1], which is why currently, research efforts are made in order to find a material model that is not only capable of correctly computing the residual stresses due to welding, but also of determining their potential relaxation as a result of cyclic loading.

This work is dedicated to the experimental analysis of the residual stress state in butt-welded ferritic-pearlitic steel pipes, which will later be used to validate the results of numerical computations. Tubular welds were chosen for this purpose because they reflect the character of actual components much better than plates. In further studies, the relaxation of the residual stresses due to cyclic loading will be investigated both experimentally and numerically. Eventually, a reliable computation of the stabilized residual stress state may allow the improvement of current fatigue design codes [2, 3], which so far do not consider relaxation effects.

A second but not less important aspect of this study is the systematic experimental investigation of the mechanisms that cause residual stresses in tubular welds, which are commonly found in engineering structures. While most of the studies on that topic found in the literature concentrate on austenitic stainless steel, see e.g., [4–6], some also exist which deal with steels where phase transformations can occur, e.g., [7–10]. In this work, the ferritic-pearlitic steel S355J2H+N is considered which is commonly used in constructions and is subject to phase transformations when exposed to high temperatures as they occur during welding. That is, the residual stresses in the welded joints investigated here are always a result of both hindered thermal contraction and impeded volume expansion caused by phase transformation. As the residual stress development due to these mechanisms has been investigated thoroughly for welded plates of ferritic-pearlitic steels [11], the results of the residual stress analysis performed on the tubular welds can be compared to the residual stress state in plane welds. To this end, plates are welded with the same parameters

---

Doc. IIW-2542, recommended for publication by Commission X  
“Structural Performances of Welded Joints — Fracture Avoidance”.

---

N. Hempel (✉) · T. Nitschke-Pagel · K. Dilger  
Institute of Joining and Welding, TU Braunschweig, Langer Kamp 8,  
38106 Braunschweig, Germany  
e-mail: n.hempel@tu-braunschweig.de

as the pipes and similarities and fundamental differences are identified.

## 2 Experimental work

### 2.1 Welding experiments

Welding experiments were performed on ferritic-pearlitic steel tubes of S355J2H+N with a specimen geometry as shown in Fig. 1. The specimens were machined on the outer and inner surface in order to remove the rolling skin and geometrical imperfections of the tubes, resulting in an outer diameter of 101 mm and a wall thickness of 8 mm. As a weld preparation, a v-shaped groove was introduced at half-length, while a thin link between the two halves of the specimen remained, preventing their misalignment and guaranteeing well-defined clamping conditions. In order to remove residual stresses due to the production or the machining of the pipes, the specimens were stress relieved thermally at 600 °C for 30 min and cooled uniformly at about 1 °C/min.

The specimens were metal active gas (MAG) welded with the filler metal G 46 4 M G4Si1 in flat position using a rotary table. Two passes were applied at room temperature (i.e.,  $T_p = T_i = 22$  °C) with nominal energy inputs of 11 kJ/cm for the root pass and 10.5 kJ/cm for the second pass. Both passes were welded in the same direction, the second pass being slightly offset. Temperature measurements were performed in the vicinity of the weld with Ni/CrNi thermocouples (type K) that were placed close to the weld toe and in the heat-affected zone (HAZ) at locations in every 90° along the specimen's circumference.

After welding, micrographs were prepared in order to determine the microstructure and the hardness in the weld seam and the HAZ. The hardness distribution was determined by the Ultrasonic Contact Impedance (UCI) method.

A comparative study was performed on S355J2 steel plates of 320×200 mm<sup>2</sup> size with the same thickness and weld

preparation, see Fig. 2. The specimens were stress relieved and butt-welded with two passes, using the same parameters as for the pipes, while being clamped at one corner.

### 2.2 Residual stress analysis

The residual stresses in the vicinity of the welds were determined by X-ray diffraction (XRD). Residual strains were measured with an  $\Omega$ -diffractometer by analyzing the shift of Cr- $K_\alpha$  radiation interference lines originating from {211} lattice planes of ferrite, bainite, or martensite. The X-ray tube voltage and current were set to 35 kV and 30 mA, respectively. The diameter of the collimator was 2 mm. At each measuring point, interference lines were recorded at eight tilt angles  $\psi$  of 0°, 13°, 18°, 27°, 33°, 39°, 42°, and 45° in a  $2\theta$  interval of 151 to 161°. The shift of the interference line's center of gravity was analyzed with the  $\sin^2\psi$  method and used to compute the residual strains, which in turn yielded the residual stresses by means of the X-ray elastic constants  $s_1 = -1.33 \cdot 10^{-6}$  mm<sup>2</sup>/N and  $s_2/2 = 6.08 \cdot 10^{-6}$  mm<sup>2</sup>/N. The average penetration depth of the X-rays was about 5  $\mu$ m.

The residual stresses were determined at points that were arranged along lines perpendicular to the welding direction. Both the longitudinal and the transverse residual stresses with respect to the welding direction were studied within a range of up to 40 mm on both sides of the weld centerline. In the weld seam and the HAZ, the distance between two measuring points was 1 mm due to the expected stress gradients in these areas. At a greater distance from the centerline, measuring points were set every 2 to 5 mm.

In case of the tubular specimens, the longitudinal and transverse residual stresses are referred to as hoop and axial stresses, respectively. Measurements were taken on the inner and outer surfaces of the pipes at every 90° along the specimens' circumference, see Fig. 3. In Fig. 3, a cylindrical coordinate system is introduced with the circumferential angle  $\phi$ , marking welding start and welding direction, and the axial coordinate  $x$  that specifies the distance from the weld centerline. The inner surfaces could only be accessed after sectioning the tubes into four quarters. To this end, the pipe was cut along lines parallel to the longitudinal axis, offset by 45° to the measuring lines. The residual stresses released by that process were monitored by strain gage measurements as well as by repeated measurements on the outer surface. In order to study the influence of the tubular geometry on the development of residual stresses, a strip of 8 mm width was cut from one of the quarters and residual stress analyses were performed on the outer surface.

Analogously, the residual stresses in a plate were determined along a line at 80-mm distance from the welding start at the top and bottom surface. Although the bottom surface was easily accessible, the plate was also cut into quarters; then,

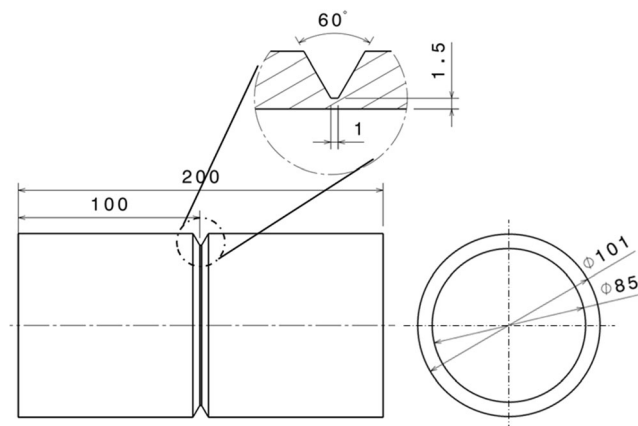
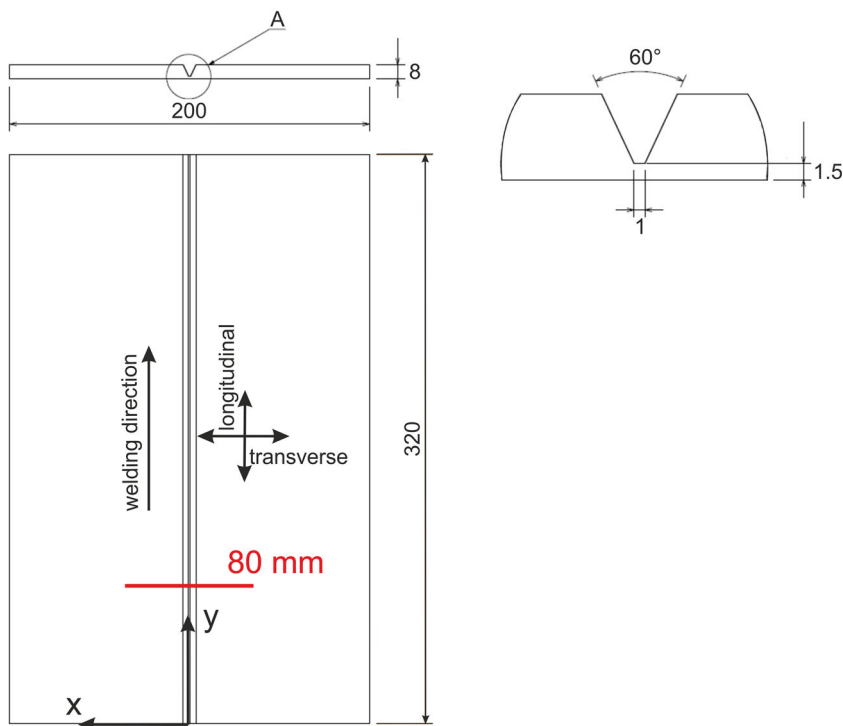


Fig. 1 Tubular specimen geometry

**Fig. 2** Plane specimen geometry and location of XRD measurements at  $y=80$  mm



the quarter at  $y=80$  mm was reduced to a strip of 8 mm width. After each step, residual stress analyses were performed.

Both for the tubular specimens and for the plate, the distortion was determined by laser triangulation after welding and after each sectioning step.

### 3 Experimental results

#### 3.1 Characterization of the welded joints

Figure 4 shows a micrograph taken at  $\phi=135^\circ$ , where the typical microstructure of a multi-pass welded ferritic-pearlitic steel can be seen with different zones of cast structure, fine and coarse grain. The hardness distribution is depicted in Fig. 5. The highest hardness values are found in

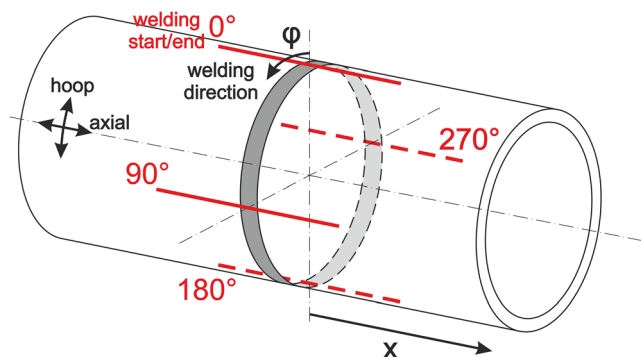


**Fig. 3** Cylindrical coordinate system and locations of XRD measurements

the HAZ, especially in the vicinity of the weld toe near the outer surface, where almost 300 HV1 are reached.

#### 3.2 Residual stress state in tubular specimens

The results of the XRD measurements taken from a tubular specimen are shown in Figs. 6, 7, 8, and 9. The stress accuracy is exemplarily given for each measuring point at  $\phi=180^\circ$ .

On the outer surface, the curves representing the hoop residual stresses at the different circumferential angles depicted in Fig. 3 are all w-shaped and, with the exception of  $\phi=0^\circ$ , almost coincide, see Fig. 6. In the weld seam, tensile stresses

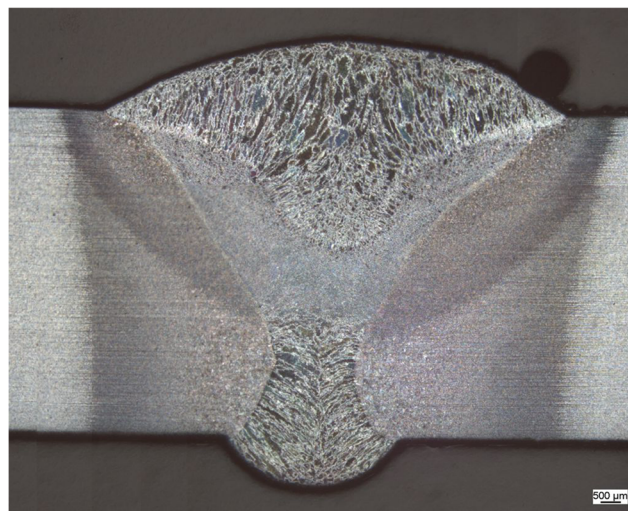


**Fig. 4** Micrograph taken from a tubular butt-weld at  $\phi=135^\circ$

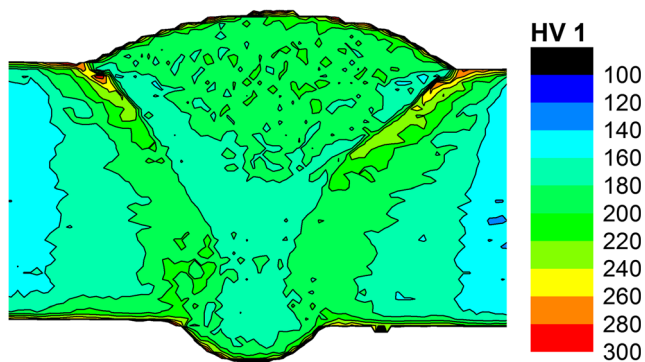


Fig. 5 Hardness distribution in the vicinity of a tubular butt-weld at  $\phi=135^\circ$

of up to 300 MPa can be found, while compressive stresses of about  $-200$  MPa occur in the base material. Near the weld toe, local minima with adjacent maxima in the base material can be observed, differing by about 50–100 MPa.

The hoop residual stress curves on the inner surface, see Fig. 7, exhibit maximum tensile stresses in the base material within a few millimeters from the weld toe, with the highest stresses at  $\phi=180^\circ$ . It should be noted that a strain gage measurement at  $\phi=200^\circ$  and  $x=8$  mm revealed a decrease of stress of about 90 MPa due to sectioning of the pipe, meaning that the original stresses were even higher. Within the weld seam, the residual stresses are about 100 MPa lower than in the adjoining base material. At about 12 mm from the weld centerline, the stresses become compressive and reach a global minimum at a distance of 20 mm. The lowest stress magnitudes can be found at  $\phi=0^\circ$ .

In axial direction, the residual stress curves on the outer surface are also w-shaped, see Fig. 8. They exhibit characteristic minima, i.e., compressive stresses, in the HAZ exceeding an absolute value of 400 MPa and thereby the yield strength of the base material of about 355 MPa. In the weld seam, the axial residual stresses are of rather low magnitude, resulting in steep stress gradients at the weld toe. In the base material, the

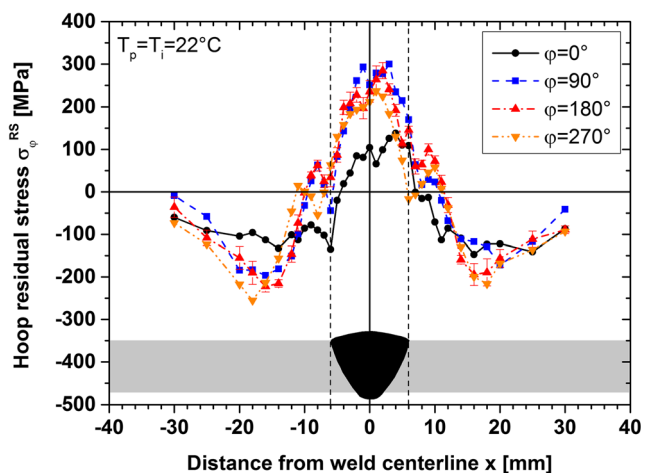


Fig. 6 Hoop residual stresses on the outer surface of an S355J2H+N pipe

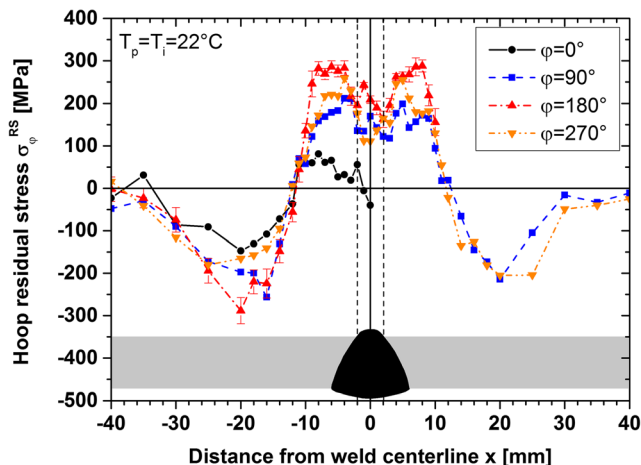


Fig. 7 Hoop residual stresses on the inner surface of an S355J2H+N pipe after sectioning

compressive stresses decrease with increasing distance from the weld toe and eventually become tensile, reaching up to 100 MPa.

The axial residual stresses on the inner surface show an opposite behavior, as can be seen in Fig. 9: tensile residual stresses are found in the HAZ and in the base material close to the weld bead, decreasing until they reach the compressive regime at about 20 mm from the weld centerline. In the weld bead, the residual stresses almost vanish completely. Again, the original stresses before sectioning the pipe have been higher in magnitude. A strain gage measurement at  $\phi=200^\circ$  and  $x=11$  mm showed that tensile stresses of 110 MPa were released.

### 3.3 Residual stress and deformation analysis of sectioned pipes and plates

Figures 10 and 11 depict the hoop and axial residual stresses, respectively, at  $\phi=90^\circ$  on the outer surface before and after sectioning the pipe into four quarters, as well as after cutting

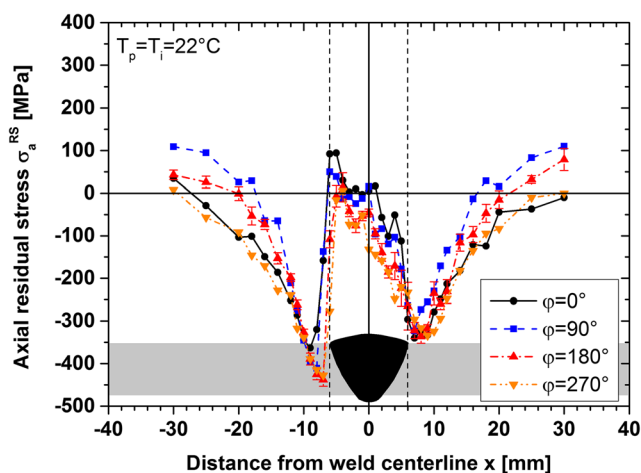
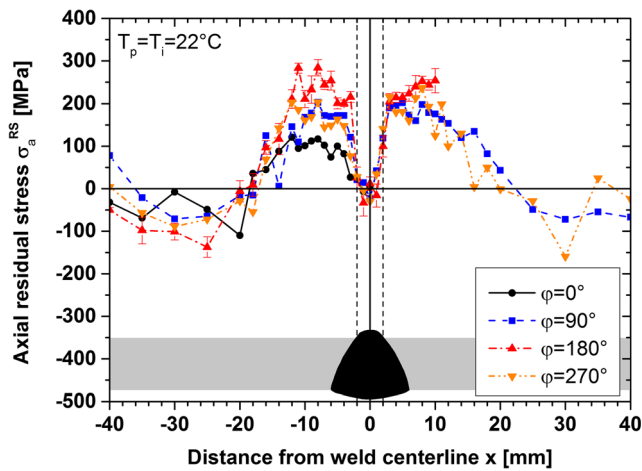


Fig. 8 Axial residual stresses on the outer surface of an S355J2H+N pipe





**Fig. 9** Axial residual stresses on the inner surface of an S355J2H+N pipe after sectioning

the quarter into a strip of 8 mm width. While the shape of the curves qualitatively remains the same after sectioning into quarters, the absolute stress values diminish significantly. The maximum hoop stress in the weld seam was reduced by about 150 MPa and the axial stress at the distinct minima in the HAZ has increased by 200–300 MPa. Moreover, the tensile axial stresses found at a greater distance from the weld centerline have vanished completely, except for a small area at about  $x = -20$  mm. When the size of the sectioned piece of material is further reduced to a width of 8 mm, the magnitude of the stress decreases even more and only vestiges of the former shape of the stress curve can be identified. At the weld centerline, the hoop stress now takes compressive values of about  $-100$  MPa.

The results of the comparative study on a welded plate are shown in Figs. 12 and 13, where the longitudinal and transverse stresses at  $y = 80$  mm on the top surface of the plate are depicted. The longitudinal stress in the unsectioned plate reaches absolute maxima of about 500 MPa in the HAZ. In

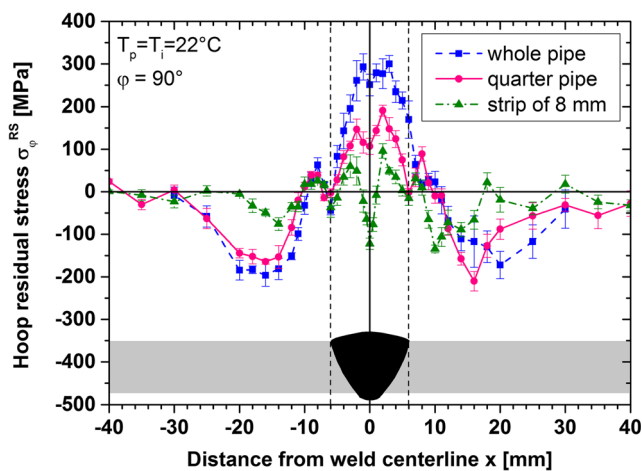


**Fig. 10** Hoop residual stresses at  $\phi = 90^\circ$  on the outer surface of an S355J2H+N pipe before and after sectioning

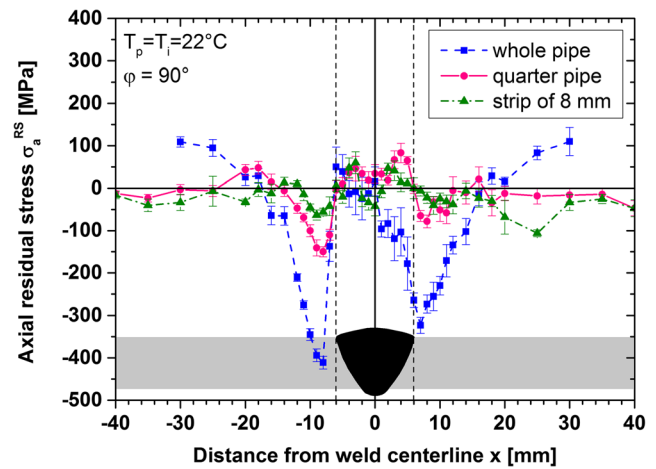


**Fig. 11** Axial residual stresses at  $\phi = 90^\circ$  on the outer surface of an S355J2H+N pipe before and after sectioning

the weld seam, the residual stress is about 100–150 MPa lower. At a greater distance from the weld centerline, the stress asymptotically approaches zero. When the plate is cut to a quarter of its original length, the longitudinal stress curve is merely shifted downwards by 200 MPa. However, the difference between the stress in the weld seam and in the HAZ has increased to 250 MPa. After cutting the quarter plate into a strip of 8 mm width, the longitudinal stress maxima are much less pronounced. In the weld seam, the stress takes compressive values of almost  $-200$  MPa.

The absolute magnitude of the transverse stress determined in the unsectioned plate is less than 70 MPa. The curve exhibits two characteristic minima in the HAZ, where the stress reaches  $-60$  MPa. Sectioning of the plate mainly results in a gradual shift of the transverse stress into the compressive regime, which is most pronounced in the base material. The minima in the HAZ, however, remain constant.

In addition to the residual stress analyses, the resulting surface profiles of both pipes and plates after welding and after

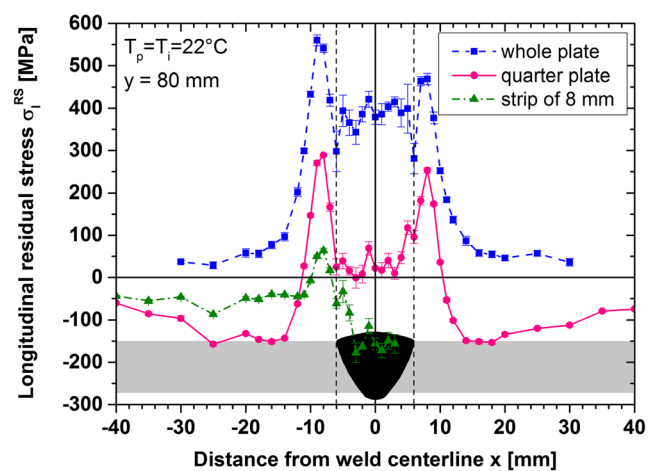


**Fig. 12** Longitudinal residual stresses at  $y = 80$  mm on the top surface of an S355J2 plate before and after sectioning

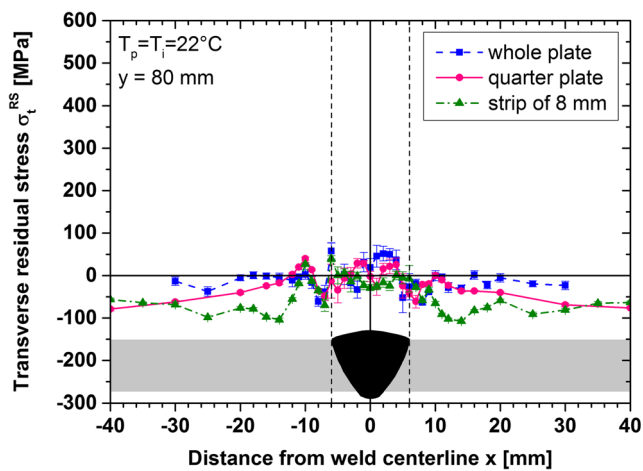


**Fig. 13** Transverse residual stresses at  $y=80$  mm on the top surface of an S355J2 plate before and after sectioning

making the respective cuts are shown in Figs. 14 and 15, respectively. It can easily be seen that welding causes a large angular distortion of the plate which is not observed for the welded pipe. Here, the area around the weld seam is shifted towards the center of the pipe, while the profile asymptotically approaches a virtual horizontal line with increasing distance from the weld seam, which is illustrated by the dotted line in Fig. 14. When the pipe is sectioned, the base material is bent downwards about the weld seam, which occurs to an even bigger extent when the small strip is cut from the pipe. Conversely, sectioning the plate has almost no effect on the deformation; the angular distortion decreases only slightly.

The temperature measurements on the pipes and plates during welding revealed similar cooling times from 800 to 500 °C,  $t_{8/5}$ , for both specimen geometries. The  $t_{8/5}$  times taken from the thermocouples closest to the weld bead range from 14 to 18 s, with  $t_{8/5}$  times of the plates rather being at the lower end and  $t_{8/5}$  times of the pipes rather being at the upper end of that interval. It could also be observed that the  $t_{8/5}$  times

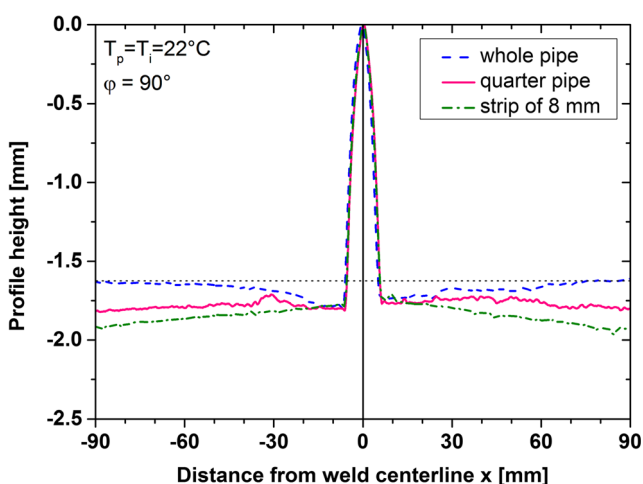


**Fig. 14** Surface profiles at  $\varphi=90^\circ$  on the outer surface of an S355J2H+N pipe before and after sectioning

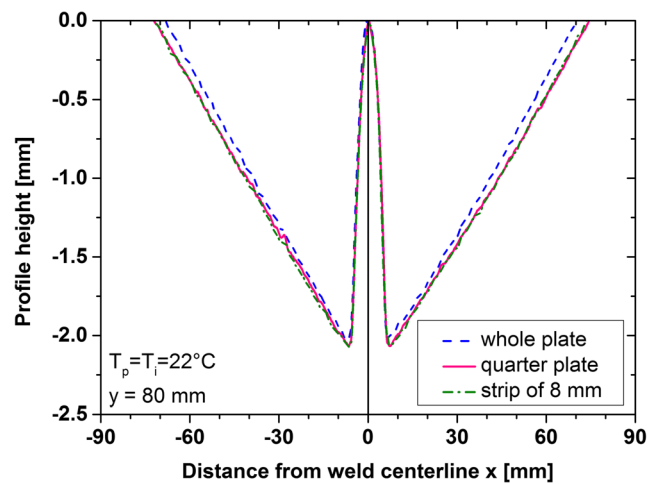


**Fig. 15** Surface profiles at  $y=80$  mm on the top surface of an S355J2 plate before and after sectioning

of the pipes increase slightly with the circumferential angle  $\varphi$ , i.e., with increasing welding time.

## 4 Discussion

### 4.1 Residual stress state in tubular specimens compared to welded plates

Although the same welding parameters are used and similar cooling times  $t_{8/5}$  are obtained, the residual stress state in welded tubular joints clearly differs from the one found in butt-welded plates. In the hoop direction, i.e., longitudinal to the welding direction, tensile residual stresses occur in the weld seam due to thermal contraction, being restrained by the adjoining base material which has a significantly lower temperature when the cooling process starts. The compressive stresses in the base material are also caused by this mechanism due to equilibrium reasons. This is valid for the hoop residual stresses both on the outer and the inner surface, see Figs. 6 and 7. On the outer surface, local minima and maxima were found near the weld toe which hint at phase transformations occurring in the weld seam and the HAZ. During cooling after welding the second pass, austenite transforms into bainite or martensite, causing a volume expansion that is impeded by the surrounding material and thus causes compressive stresses in the weld seam and tensile stresses in the base material. The residual stress state resulting from phase transformations is superposed by the residual stresses due to hindered thermal contraction, leading to the distributions seen in Figs. 6 and 7.

The same mechanisms are responsible for the development of longitudinal residual stresses in welded plates, see [11]. The fact that no compressive longitudinal stresses were found in the base material of the plates in this study can be explained by bending about the  $x$ -axis of the plates due to shrinkage of the

multi-pass weld seam, causing additional tensile stresses on the top surface.

While the hoop residual stresses in the tubular welds are similar to the longitudinal stresses in plates, this is not the case for the axial residual stresses, i.e., the stresses transverse to the welding direction. Most noticeably, high compressive stresses occur near the weld toe, see Fig. 8, which can only be found to a minor degree in welded plates, see Fig. 13. The significant difference can be explained by the tubular geometry. During cooling, the weld seam contracts in circumferential direction, thereby also causing a radial contraction or necking of the pipe, which was revealed by the deformation measurements whose results are shown in Fig. 14. Here, the dashed line represents the undeformed surface of the pipe so that the radial contraction can easily be identified. The consequent bending of the pipe wall causes axial stresses which, at the outer surface, are compressive in the vicinity of the weld seam and tensile at distances of about  $|x| > 20$  mm, see Fig. 8. Typical of bending, this pattern is reversed at the inner surface where the residual stresses are tensile near the weld seam and compressive for  $|x| > 20$  mm, cf. Fig. 9. Within the weld seam, the bending stresses are superposed by stresses due to hindered thermal contraction, which results in almost negligible axial stresses both on the outer and on the inner surface. Similar distributions of the axial residual stress were found for TIG dummy welds on pipes of S355J2H and S690QL [12]. Moreover, bending has also been identified as the main mechanism causing axial stresses in austenitic steel pipes [5].

The fact that the compressive stresses at the outer surface exceed the yield strength of the base material, which has been determined to be about 355 MPa by tensile tests, can be explained by a high amount of martensite in the HAZ near the surface, where the cooling rate is the highest. This leads to an increased yield strength and the high hardness values shown in Fig. 5.

In welded plates, the transverse residual stresses are of rather low magnitude because the degree of constraint is much lower than for pipes, which results in the large angular distortion observed in Fig. 15. The fact that stress minima near the weld toe can also be found in welded plates hints at phase transformations occurring during cooling [11]. Therefore, it can be inferred that phase transformations also contribute to the distinct stress minima in welded pipes. This point will also be addressed in the next section.

The stress curves determined at different circumferential angles of the pipes differ only slightly, with the exception of the residual stresses at  $\varphi = 0^\circ$  which might be affected by the fact that this area is heated twice for every weld pass.

The fact that slightly longer cooling times  $t_{8/5}$  have been observed for welded pipes in comparison to plates can be explained by the specimen geometry. While the welding path is linear for plates, each welding pass forms a closed loop in the case of girth-welded pipes. Therefore, the heat introduced

by the welding process can spread more easily within a pipe than within a plate, e.g., also flowing in the opposite direction of the welding direction and thus heating parts of the specimen that have not been welded yet. With increasing welding time, this effect gets more pronounced, which is shown by the fact that the  $t_{8/5}$  times are longer at higher circumferential angles  $\varphi$ .

#### 4.2 Influence of sectioning welded pipes and plates

In general, the magnitude of the residual stresses decreases as the size of a section cut from a pipe is reduced, as shown in Figs. 10 and 11. When the pipe is cut into quarters, its self-constraining tubular geometry is disturbed significantly. Even though the hoop residual stresses on the outer surface are only slightly influenced, which means that the impeded circumferential contraction of the weld seam is still present, the magnitude of the axial stress minima at the weld toes and the tensile axial stresses at distances of more than 20 mm from the weld centerline have decreased significantly. This is due to the lowered degree of geometrical constraint, allowing the pipe section's endings to bend downwards and the axial residual stresses to be released to a large extent. Simultaneously, it can be observed that the necking of the pipe in the vicinity of the weld seam, which has been clearly visible for the unsectioned pipe, is less pronounced, see Fig. 14.

The significance of the tubular geometry becomes even more obvious when the sectioning process of a welded plate is compared. The transverse residual stresses, as well as the angular distortion, remain almost unchanged when a quarter is cut from the plate, see Figs. 13 and 15, which is due to the fact that the plane geometry is not modified substantially by the cut. The shift of the longitudinal residual stresses, which is shown in Fig. 12, can be explained by the fact that the transverse bending about the  $x$ -axis, causing longitudinal stresses at the top surface of the plate, has decreased because of the shorter length of the remaining plate section.

When the pipe section is reduced to an 8-mm-wide strip, the influence of the tubular geometry is almost completely removed and the surface profile does not show any necking anymore, see Fig. 14. The magnitude of the remaining axial residual stresses has decreased even more, see Fig. 11. However, the stress minima near the weld toe still exist, even though they are reduced to about  $-50$  MPa. Compared to cutting the pipe into quarters, the hoop residual stress now has significantly changed as well because the cutting surfaces, where the hoop stress must be zero, are only a few millimeters away. Thus, the circumferential contraction of the weld seam is only constrained to a minor degree and a new equilibrium is established, where even compressive hoop stresses can occur in the weld seam, see Fig. 10.

Similarly, when an 8-mm-wide strip is cut from the plate, the transverse stress minima of about  $-60$  MPa near the weld

toe remain unchanged, as seen in Fig. 13. Since these are ascribed to phase transformations [11] and also occur in the strip cut from a pipe, it can be inferred that the hindered volume expansion due to phase transformations indeed contributes to the residual stress state found in pipes and thus to the distinct minima of axial residual stress near the weld toe. However, the similar magnitude of the transverse stress minima in the strips of both pipes and plates does not automatically mean that residual stresses due to phase transformations play a minor role in the development of residual stresses in the tubular welds considered in this study. It should be noted that pipes are subject to a much higher degree of constraint than plates, which, for instance, is seen in the large angular distortion of the welded plates. The same mechanism can therefore cause higher stresses in pipes. When the influence of the tubular geometry and thus the degree of constraint is reduced by sectioning, the axial residual stresses both due to wall bending and due to phase transformations decrease.

On the other hand, it has been found in a previous study that a preheating temperature of 150 °C and an interpass temperature of 300 °C did not qualitatively alter the residual stress distributions in the type of tubular welds analyzed here [13]. Even though the cooling time  $t_{8/5}$  was distinctly longer, which usually leads to a reduction of the influence of phase transformations and thus to higher tensile residual stresses [11], the same stress maxima and minima were found as in this study, only with a decreased magnitude. While the latter point can be explained by the smaller temperature difference between base material and weld metal due to the preheating, the first point reveals that phase transformations play only a minor role in the development of welding residual stresses in the ferritic-pearlitic steel pipes investigated here. Instead, the governing mechanism is the circumferential contraction, causing necking and wall bending, thus, providing an axial residual stress state that differs distinctly from the transverse one in welded plates.

In the literature, different results concerning the influence of phase transformations on the development of residual stresses on welded pipes are reported. For instance, Jonsson and Josefson discovered that analytical solutions not taking account of phase transformations could approximate experimentally determined residual stresses in a single-pass tubular weld quite well [10]. Deng and Murakawa, however, reached a different conclusion for pipes of two different steels where phase transformations play a decisive role [7, 8].

Sectioning is a necessary requirement for performing residual stress analyses by XRD on the inner surface of the tubular specimens. However, as it affects the residual stress state, the stresses determined on the inner surface after sectioning are not the ones that would have been found in the original state of the pipe. Both the XRD measurements performed at the outer surface before and after sectioning and the strain gage analyses on the inner surface suggest that the residual stresses decrease due to the sectioning process, meaning that the tensile

stresses both in hoop and axial direction on the inner surface were originally higher than shown in Figs. 7 and 9.

## 5 Summary and conclusions

The residual stress state on the inner and outer surfaces of butt-welded pipes of the ferritic-pearlitic steel S355J2H+N has been investigated by X-ray diffraction and compared to the one in plates welded with the same parameters. In general, the mechanisms causing residual stresses, hindered thermal contraction and phase transformations, occur in both pipes and plates. However, it was shown that the self-constraining tubular geometry causes a stress state significantly different from the one found in plates. This holds especially for the stresses transverse to the weld seam, i.e., in axial direction of the pipes, which are distinctly compressive on the outer surface and tensile on the inner surface of the pipes. The governing mechanism for these effects is the circumferential contraction of the weld seam, causing a necking of the pipes and therefore bending of the pipe wall. Phase transformations in the weld seam and the HAZ contribute to the residual stress state but play only a minor role in the welds considered in this study. However, they allow higher stresses in the HAZ due to the production of martensite which has a higher yield strength than the base material. More information about the contribution of the phase transformations may be deduced from experiments using a lower heat input in order to maximize the influence of phase transformations or from investigations of austenitic steel pipes with a similar geometry, where phase transformations do not occur.

The residual stress state found in the present study may have practical implications for the fatigue and fracture performance of these joints. Since the highest tensile axial residual stresses occur near the weld toe at the inner surface, fatigue cracks will supposedly be initiated at these sites, when the pipes are loaded axially. Investigations of the fatigue behavior of the tubular joints due to cyclic bending will be carried out in a later study.

**Acknowledgments** We would like to thank the German Federation of Industrial Research Associations (AiF) for their financial support of the research project IGF No. 17.619N. This project was carried out under the auspices of AiF and financed within the budget of the Federal Ministry for Economic Affairs and Energy through the program to promote joint industrial research and development (IGF).

## References

1. Wohlfahrt H, Nitschke-Pagel T, Dilger K, Siegele D, Brand M, Sakkietitbutra J, Loose T (2012) Residual stress calculations and measurements – review and assessment of the IIW round robin results. *Weld World* 56 No. 09/10:120–140



2. Hobbacher A (2007) Recommendations for Fatigue Design of Welded Joints and Components. IIW-Document, XIII-2151-07 / XV-1254-07
3. (2005) EN 1993-1-9 (Eurocode 3): Design of Steel Structures, Part 1.9: Fatigue, CEN, Brussels, Belgium
4. Bouchard PJ (2007) Validated residual stress profiles for fracture assessments of stainless steel pipe girth welds. *Int J Press Vessel Pip* 84:195–222
5. Deng D, Murakawa H, Liang W (2008) Numerical and experimental investigations on welding residual stress in multi-pass butt-welded austenitic stainless steel pipe. *Comput Mater Sci* 42:234–244
6. Yaghi AH, Hyde TH, Becker AA, Sun W, Williams JA (2006) Residual stress simulation in thin and thick-walled stainless steel pipe welds including pipe diameter effects. *Int J Press Vessel Pip* 83:864–874
7. Deng D, Murakawa H (2008) Finite element analysis of temperature field, microstructure and residual stress in multi-pass butt-welded 2.25Cr–1Mo steel pipes. *Comput Mater Sci* 43:681–695
8. Deng D, Murakawa H (2006) Prediction of welding residual stress in multi-pass butt-welded modified 9Cr–1Mo steel pipe considering phase transformation effects. *Comput Mater Sci* 37:209–219
9. Yaghi AH, Hyde TH, Becker AA, Williams JA, Sun W (2005) Residual stress simulation in welded sections of P91 pipes. *J Mater Process Technol* 167:480–487
10. Jonsson M, Josefson BL (1988) Experimentally determined transient and residual stresses in a butt-welded pipe. *J Strain Anal Eng* 23: 25–31
11. Nitschke-Pagel T, Wohlfahrt H (1992) Residual stress distributions after welding as a consequence of the combined effect of physical, metallurgical and mechanical sources. In: Karlsson L, Lindgren LE, Jonsson M (eds) *Mechanical effects of welding*, IUTAM symposium Lulea/Sweden 1991. Springer Verlag, Berlin, pp 123–134
12. Farajian M, Nitschke-Pagel T, Dilger K (2013) Welding residual stresses in tubular joints. *Mater Sci Forum* 768–769:605–612
13. Hempel N, Nitschke-Pagel T, Dilger K (2014) Residual stresses in multi-pass butt-welded tubular joints. *Adv Mater Res* 996:488–493